Molecular Dynamics Study of Water−Acetonitrile Mixtures

Raymond D. Mountain[†]

Physical and Chemical Properties Division, 100 Bureau Drive Stop 8380, National Institute of Standards and Technology, Gaithersburg, Maryland 20899-8380

Received: July 7, 1999; In Final Form: October 13, 1999

The results of a molecular dynamics simulation study of water acetonitrile mixtures over the temperature range 297−415 K are reported. The emphasis is on the microheterogeneous structure present in these mixtures for compositions ranging from 0.1−0.9 mole fraction of water. The characterization of the microstructure is presented in terms of site−site pair correlation functions and in terms of the size and shape of water clusters and acetonitrile clusters.

1. Introduction

The feasibility of using molecular dynamics simulations to investigate retention mechanisms operating in Reversed-Phase Liquid Chromatography (RPLC) has been demonstrated.[1−3] This article reports results from a series of molecular dynamics simulations that were performed to provide information on the molecular level structure for one of the mobile phases used in RPLC, namely, mixtures of water and acetonitrile.[4] It has been suggested that microheterogeneity of the solvent is a factor in the thermodynamics of the retention of nonpolar solutes when the mobile phase is a mixture of acetonitrile and water.[5] This suggestion provides an elaboration of the earlier conjecture[6] that nonelectrolyte aqueous mixture thermodynamics could be rationalized if the fluid were heterogeneous on a molecular length scale. The mixtures used in RPLC commonly contain mole fractions of water between 0% and 70% and are operated at temperatures in the 10−40 °C interval. We describe here the results of a molecular dynamics simulation study of microstructure of aqueous acetonitrile mixtures under conditions varying from 297−415 K with compositions ranging from mole fraction of 10% water to 90% water. This temperature and density range, which is somewhat wider than typical RPLC conditions, was chosen to generally explore clustering in these mixtures.[7,8]

The existence of water rich and acetonitrile rich "clusters" has been demonstrated by evaluating the Kirkwood−Buff integrals[9,10] with the use of measured thermodynamic quantities.[1,2] More recently, X-ray diffraction measurements indicate that microheterogeneity is present in the form of coexisting water and acetonitrile clusters in the mixture.[13] With molecular dynamics, we determine more detailed information about the microheterogeneity of the mixtures than is possible with these approaches.[14] Two complementary measures obtained using molecular dynamics are discussed. One is in terms of the site−site pair distribution functions. We also sample the clusters directly and obtain information on the cluster sizes in terms of the number of molecules in a cluster and on the "shape" of the clusters.

2. Simulations

With one exception, the simulations discussed here were performed with a total of 216 molecules. The mole fraction of water molecules X was varied from 0.1−0.9 in increments of 0.2. The case with $X = 0.5$ was also simulated for a larger, 1000 molecule system at ambient conditions. The equations of motion were integrated using an iterated form of the Beeman algorithm[15] with a time step of 1 fs and the temperature was controlled using separate Nosé−Hoover thermostats for the translational and orientational degrees of freedom.[16] The orientational degrees of freedom were described using quaternions.[17,18] The density used in the bulk simulations is that of the mixture at 25 °C as reported by Cunningham et al.[19] The simulations were performed for five compositions under constant volume and temperature conditions; therefore, Canonical ensemble averages and pair distribution functions were obtained. The Kirkwood−Buff integrals were not evaluated as the asymptotic behavior of the pair functions in the canonical ensemble differs from the grand canonical ensemble pair functions for which the Kirkwood−Buff theory applies.[20,21] While differences are not significant for the purposes of this paper, because the differences are inversely proportional to the number of molecules in the system, the differences make it not possible to evaluate the Kirkwood−Buff integrals using the results of these simulations.

The water and acetonitrile molecule interactions were modeled using the SPC/E model[22] and the model due to Edwards et al.,[23] respectively. Both models represent the molecules as rigid objects with three force centers. The force centers are located close to the positions of the atoms (united atom in the case of the CH_3 group in acetonitrile) in the molecules. These models have been shown to provide realistic representations of the thermal properties of the liquid.[22,24] In each model, the intermolecular interactions are represented as a sum of Coulomb interactions plus Lennard-Jones interactions. For the mixture, we have used the usual combining rules to determine the water-acetonitrile Lennard-Jones parameters so that the diameter σ, is the arithmetic mean and the energy parameter ϵ is the geometric mean respectively of the water−water and acetonitrile−acetonitrile parameters. The specific values are listed in Table 1, as are the charges on the sites.

The charges on the molecules are "effective charges" since the induced charges resulting from the field of neighboring molecules are included in a mean-field sense.[22,25] No adjustment in the charges has been made here although the molecular environment in a mixture is different from that in the pure liquid.

[†] E-mail: Raymond.Mountain@nist.gov.

10.1021/jp992305+ CCC: $18.00
Published on Web 11/18/1999

TABLE 1: The Lennard-Jones Parameters for the Mixture[a]

sites	ϵ/K_B, K	σ, nm
O−O	78.24	0.3166
Me−Me	191.0	0.4392
C−C	50.0	0.3400
N−N	50.0	0.3299
Me−C	97.41	0.3499
Me−N	97.41	0.3452
C−N	50.0	0.3350
Me−O	122.3	0.3382
C−O	62.55	0.3283
N−O	62.55	0.3232

[a] O and H stand for the oxygen and hydrogen sites on the water molecule and Me, C, and N stand for the methyl, carbon, and nitrogen sites on the acetonitrile molecule. For these models, there is no Lennard-Jones interaction involving the H-sites. In units of the charge on the proton, the charge on the O-site is −0.8476 and on the H-site is 0.4238. The charge on the Me-site is 0.2690, on the C-site is 0.1290, and on the N-site is −0.3980.

The additional effort needed to explicitly include polarizability in the molecular description is not warranted at this time given the low level of understanding of how to do this in a way that improves the description beyond the mean-field level.[26,28] Thus, a note of caution about our results is in order. The results should be viewed as providing a qualitative description of the composition and temperature variation of the structure of the liquids.

Considerable care was taken to ensure that the structure of the mixture was not influenced by the initial conditions. This was done by making a stabilization run of 100 ps duration before any production runs were made. The production runs were also of 100 ps duration. In some of the low temperature cases, a second production run was made to verify the stability of the results.

Also, two separate runs for the 1000 molecule, equimolar mixture were performed starting from quite different initial conditions. In the first case, the initial condition had two slabs of fluid in contact. One slab contained 500 water molecules, and the other slab contained 500 acetonitrile molecules. In the second case, each molecule had six unlike molecules as near neighbors. After stabilization runs of 300 ps duration, the two cases developed equivalent clustering.

Two sets of simulations were performed for the water acetonitrile mixtures. One set was for isolated droplets of the mixture. These simulations illustrate the tendency of water clusters to reside in the interior of the actonitrile cluster. The temperature of the droplets was maintained at 297 K. The droplets were confined to a spherical region of 3 nm about the center of mass of the droplet by a softly repulsive potential. The molecules interacted with this wall potential only when a molecule was more than 2.6 nm from the center of the droplet. This proved to be a quite rare event for this size droplet at this temperature so the confining potential had little influence on the properties of the droplet.

The second set of simulations were for the bulk mixtures. In these simulations, periodic boundary conditions were imposed. The long-range part of the Coulomb interaction was obtained using the Ewald summation method.[29] These were more extensive simulations as three temperatures, 297, 313, and 415 K, were examined. The first two temperatures are in the region used in RPLC and the third temperature is where the second neighbor coordination of water has become markedly less tetrahedral than it is at the lower temperatures.

One characterization of microheterogeneity is in terms of clusters of molecules. Two molecules are said to be in a cluster if the distance between them is less than the position of the first minimum in the pair correlation function for the molecules in question. This distance is 0.341 nm for water clusters and 0.647 nm for acetonitrile clusters. With this cluster rule, it is a simple task to identify the clusters in a sample.[30] This cluster rule will identify clusters that are larger than clusters based on a hydrogen bonding rule.[14,31] During a run, statistics for water clusters and for acetonitrile clusters were gathered every 10 time steps. The number of molecules in each cluster and the principal moments of inertia of each cluster were recorded.

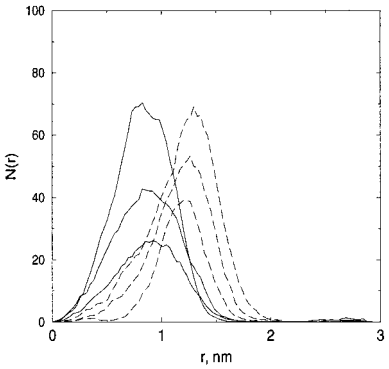

Figure 1. The number density profiles for the water molecules, solid lines, and for the acetonitrile molecules, dashed line, are shown for $X = 0.3$, $X = 0.5$, and $X = 0.7$ for $T = 297$ K. The mole fraction X increases for the curves moving up for the solid lines and down for the dashed lines.

The moments of inertia were obtained by constructing the inertia tensor for the cluster,[32]

$$\mathcal{T}_{\alpha\beta} = \frac{1}{N_c}\sum_{i=1}^{N_c}[\delta_{\alpha\beta} r_i^2 - x_i^\alpha x_i^\beta]$$

where molecule i is located a distance $\mathbf{r}_i$ from the center of mass of the cluster containing N_c molecules and x_i^α is the alpha-component of $\mathbf{r}_i$. The eigenvalues of this tensor, $R_1^2 \le R_2^2 \le R_3^2$, are the principal moments of inertia of the cluster. Another characterization of microheterogeneity is through the pair distribution functions. A total of 15 site−site pair functions exist for these three-site models of water acetonitrile. For the bulk simulations, the normalization convention used is that the site−site pair functions approach "unity" in the Canonical ensemble sense[20] for large separations.[33] Other conventions have been used when discussing molecular correlations in liquids so it is important to specify clearly how the functions are normalized.[33,35] The correlation functions for isolated droplets are proportional to the probability of finding a pair with the specified separation and no other scaling of the functions was imposed.

3. Results, Isolated Droplets

First we briefly examine the internal structure of isolated droplets of water acetonitrile mixtures at 297 K. Five compositions were studied for $X = 0.1$, 0.3, 0.5, 0.7, and 0.9 with a total of 216 molecules in each droplet.

The resulting number density profiles are illustrated in Figure 1 for the droplets with X = 0.3, 0.5, and 0.7. In each case, the water molecules *tend* to be inside the acetonitrile molecules. The formation of an acetonitrile rich surface layer at a liquid−vapor interface has been inferred from sum frequency infrared measurements for water acetonitrile mixtures.[36] The pair functions for molecules in the droplet are similar, but not identical, to those for molecules in bulk. Both sets of functions show oscillations of decreasing amplitude as the separation of the pairs increases. In the bulk, there is a finite large separation limiting

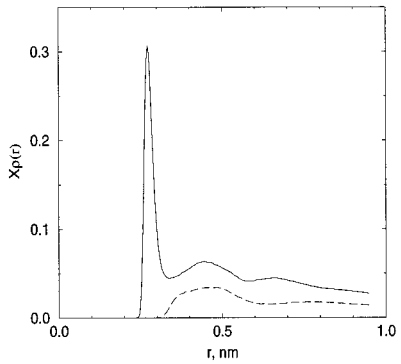

Figure 2. The composition weighted pair density distribution functions for water (solid line) and for acetonitrile (dashed line) are shown for a droplet containing 216 molecules at $T = 297$ K with $X = 0.5$.

value while in the droplet, the limiting value is necessarily zero. Figure 2 shows the droplet pair functions for $X = 0.5$.

The water clusters and the acetonitrile clusters in isolated droplets are not spherical objects. Rather they are extended, somewhat interpenetrating collections of molecules. For $X = 0.1$, the water molecules are dispersed in small sets of seven or fewer molecules in a cluster while the acetonitrile molecules are in one large cluster.

The water clusters increase in size as X increases while the acetonitrile molecules remain in one large cluster until $X = 0.9$.

A useful way to discuss the distribution of cluster sizes is to consider the fraction of the samples that contain a cluster with at least one-half of the molecules of a particular species. In those cases, there is only one "large" cluster present in the system and the frequency of occurrence will provide an unambiguous measure of the likelihood of finding clusters of that size in the mixture. We use this terminology. If a cluster contains N molecules and there are N_T molecules of that type in the system, then the fraction of molecules in a cluster is $f_x = N/N_T$. Also the ratio of the largest eigenvalue of the inertia tensor of the cluster to the smallest eigenvalue is $R_{31} = R_3/R_1$. For $X = 0.3$, 80% of the samples have water clusters with $f_x \geq 0.9$ and $1.2 \leq R_{31} \leq 1.5$, indicating that the clusters are nonspherical. For $X = 0.5$, 90% of the clusters have $f_x \geq 0.9$ and $R_{31} \approx 1.4$. For $X = 0.7$, all of the water molecules are in a single, nearly spherical cluster with $R_{31} \approx 1.2$. At this composition the acetonitrile molecules are in a single cluster with $R_{31} \approx 1.1$. Increasing the water mole fraction to 0.9 has little effect on the water cluster but leads to a breakup of the acetonitrile into small clusters, much like water at the other end of the composition interval.

4. Results, Bulk

Now we consider the bulk simulation results. For a water−acetonitrile mixture, there are many site−site pair functions. We will restrict our attention to those functions that provide information on the microheterogeneous structure of the mixture. These are the oxygen−oxygen function $g_{OO}(r)$ for water and the carbon−carbon function $g_{CC}(r)$ for acetonitrile. For water−acetonitrile correlations, the interesting functions are the oxygen−carbon correlation function $g_{OC}(r)$ and the hydrogen−nitrogen correlation function $g_{HN}(r)$.

The pair distribution functions indicate that water clusters and acetonitrile clusters have rather different characteristics. Water forms clusters rather than experience a complete breakup of the hydrogen bond network present in bulk water. The extent of the cluster depends on the mole fraction of water in the mixture and on the temperature. The composition dependence

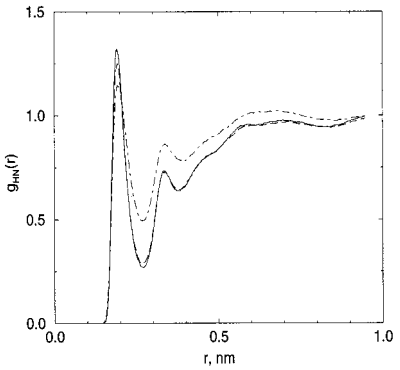

Figure 3. The hydrogen bond between water and the nitrogen site of acetontrile is indicated by the feature centered at $r = 0.19$ nm. This is for $X = 0.3$ for $T = 297$ K (solid line), 313 K (dashed line), and 415 K (long−short dashed line).

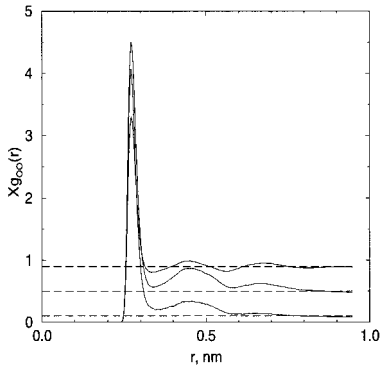

Figure 4. The composition weighted oxygen−oxygen pair functions, $Xg_{OO}(r)$, are shown for $X = 0.1$, $X = 0.5$, and $X = 0.9$ for $T = 297$ K. The dashed lines indicate the asymptotic value X for each case.

will be discussed below. The clustering tendancy decreases with increasing temperature and is generally moderated to some extent as water can form a hydrogen bond with the nitrogen site of acetonitrile.[37−39] This is indicated by a sharp maximum in $g_{HN}(r)$ located at $r = 0.19$ nm as shown in Figure 3.

There is only a small variation in this feature as a function of temperature. The $g_{OO}(r)$ functions for the $T = 297$ K states are shown in Figure 4 for the compositions $X = 0.1$, 0.5, and 0.9. The horizontal dashed lines indicate that asymptotic value of $Xg_{OO}(r)$. The strong clustering tendancy of water at low concentrations is indicated by the "approach from above" to the asymptotic value for the first three neighbor shells followed by an extended range where the correlation function lies below that value. The highest concentration case more closely resembles the pair function for bulk water. The height of the first maximum in $g_{OO}(r)$ increases strongly with decreasing water fraction. This feature has been invoked as an indication of clustering.[39] The corresponding functions for acetonitrile $(1-X)g_{CC}(r)$ show different behavior as the composition of the mixture varies. On the length scale of these simulations, there is not much departure from the bulk liquid in the shape of the functions. This is illustrated in Figure 5. This suggests that the clustering of acetonitrile implied by the clustering of water produces more spatially extended sets of molecules than is the case for water.

That suggestion is verified by examining the cluster size distributions for water and acetonitrile clusters. In a simulation, the distribution of cluster properties is most informative when clusters are sufficiently small (or the simulated system sufficiently large) that a range of sizes can be sampled. Once a cluster contains most of the molecules it is not possible to infer

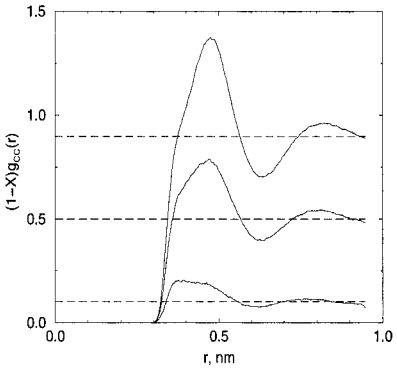

Figure 5. The composition weighted carbon−carbon pair functions, $(1\text{-}X)g_{CC}(r)$, are shown for $X = 0.1$, $X = 0.5$, and $X = 0.9$ for $T = 297$ K. The dashed lines indicate the asymptotic value, $1-X$, for each case.

the existence of an upper limit on cluster size. For the case with $X = 0.1$, there are a total of 22 water molecules in the system. For $T = 297$ K, about one-fourth of the samples have $0.5 < f_x < 0.6$ with $R_{31} \approx 1.6$. No larger water clusters were found. For $T = 313$ K, only one-tenth of the samples have $f_x \geq 0.5$ and no clusters with $f_x \geq 0.5$ are found at $T = 415$ K. The remaining water molecules form quite small clusters, mostly in the 2−5 molecule range. These objects appear to fill in vacancies present in the one large acetonitrile cluster. As the mole fraction of water increases, larger water clusters are formed.

For $X = 0.3$, there are a total of 64 water molecules. All of the samples have $f_x \geq 0.5$ for the two lower temperatures. This decreases to 40% of the samples at the high temperature. The large water clusters are moderately nonspherical with $1.3 \leq R_{31} \leq 1.6$. For this composition, all of the acetonitrile molecules are in a single cluster. For $X = 0.5$, there are 108 water molecules in the system and all of the samples have at least 90% of the water molecules in a single cluster for the lower two temperatures. This decreases at the high temperature where over 90% of the samples have at least 80% of the molecules in a single cluster. For these clusters, $R_{31} \approx 1.2$ as the clusters now span the simulation cell. Again, there is just one acetonitrile cluster.

The large system, containing 500 water molecules, has the same cluster properties as the small system. Namely, over 90% of the water molecules are in a single cluster and $R_{31} \approx 1.2$. Of course, the number of molecules in the clusters are different and this indicates that system size effects are worth considering. Snapshots of the configurations of the smaller system show that the single large cluster of water molecules is not compact. Snapshots of configurations of water molecules in the larger system reveal that the large cluster consists of fairly dense regions that are interconnected by more tenuous regions with a lower density of water molecules. Again, the cluster is not compact, even in the dense regions.

For $X = 0.7$, there are 151 water molecules in the system. We find one large water cluster and one large acetonitrile cluster, even at the highest temperature. It is only for the case with $X = 0.9$ that the acetonitrile molecules do not form a single large cluster, although all samples have at least 60% of the acetonitrile molecules in a single cluster. An alternative way of examining the clustering tendency of the mixture is in terms of the composition−composition correlation function $G_{cc}(r)$. This is the combination of correlation functions that describes the spatial composition fluctuations of mixture,[9,33] namely,

$$G_{cc}(r) = X(1-X)[1 + X(1-X)(g_{OO}(r) + g_{CC}(r) - 2g_{OC}(r))]$$

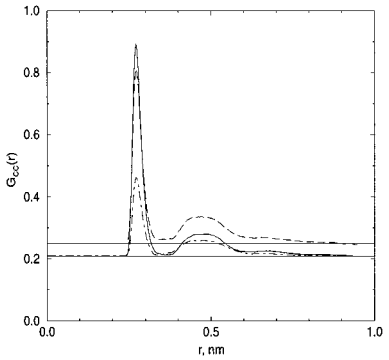

Figure 6. The composition composition correlation function at $T = 297$ K for three compositions, $X = 0.3$ (solid line), 0.5 (dashed line), and 0.7 (long−short dashed line). The first feature is due to $g_{OO}(r)$, and the second feature is due to $g_{CC}(r)$.

The oxygen and carbon sites are quite close to the centers of mass of the molecules; therefore, these functions serve as the molecule molecule correlations that appear in the fluctuation theory of mixtures. Some examples for these mixtures are shown in Figure 6. Since the correlation functions are nonnegative, any dip below the base line value $X(1 - X)$ is an indication that unlike species are ordering. That behavior is known as compositional ordering and is *not* present in these mixtures.

5. Discussion

Water−acetonitrile mixtures exhibit microheterogeneity in the form of coexisting, interpenetrating water rich and acetonitrile rich clusters over an extensive range of composition and temperature values. This feature is present both in bulk samples and in isolated droplets. When a free surface is present, as in the droplets, there is a tendency for the surface region to be acetonitrile rich. This was also found to occur when the interface was with tethered chain alkane-like molecules.[3] Presumably, this would occur unless an explicitly hydrophillic phase was present at an interface.

The variation of cluster sizes extends over a broader composition range for water than for acetonitrile. First, the water molecules are smaller than the acetonitrile molecules and the water molecules pack more closely due to the hydrogen bond network that forms. The differences in the shape of the pair functions in the first neighbor range are striking, as shown in Figures 4 and 5, and are an indication of these packing tendencies.

Another factor that influences the cluster size distribution is that the volume per molecule is considerably higher for small values of X than it is for large values of X. Other studies have shown that the size of cavities in a liquid depends mainly on the density of the liquid.[31,40,41] This means that water molecules at low concentration of water molecules can fit into naturally occurring spaces more readily than acetonitrile molecules can when the acetonitrile concentration is low.

To put this in another light, the number density of the liquid at the low water concentration region is quite low for liquid water, but normal for liquid acetonitrile. The number density at $X = 0.3$ is less than twice the critical density for pure water. The clustering tendency of pure water observed in the supercritical region.[31] is not suppressed at these lower temperatures. At the other end of the composition range, the environment experienced by the dilute acetonitrile molcules is one of an unusually high number density, making it difficult for disjoint acetonitrile clusters to exist until $1-X$ is quite small. So part of the explanation of the observed distribution of clusters sizes is one of packing.

At lower temperatures than those considered here, water acetonitrile mixtures undergo a true liquid−liquid-phase separation with an upper solution critical point at $T = 272$ K and $X = 0.62$.[42] The clustering discussed here should not be viewed just as a manifestation of critical fluctuations. Near a liquid−liquid critical point, the composition composition correlation function $G_{cc}(r)$ becomes long ranged reflecting the large composition fluctuations that occur near the critical point.[43] Figure 6 displays the composition composition correlation function at $T = 297$ K for $X = 0.3$, 0.5, and 0.7. For these compositions, the simulation cell has a repeat distance greater than 1.86 nm and the correlation lengths are on the order of 0.6−0.7 nm. Critical fluctuations would be expected to yield a greater correlation length for $X = 0.7$ and 0.5 than for $X = 0.3$. Since this is not what is found, critical fluctuations are not a useful way to describe the microheterogeneity in this mixture, at least for the temperatures and compositions examined here.

The main conclustion to be drawn from this study is that water acetonitrile mixtures exhibit microheterogeneity over a considerable range of temperatures and for compositions ranging from $X = 0.1$ to 0.9. The details of the heterogeneity depend on both temperature and composition. The type of microheterogeneity found in the range of interest in RPLC has a broad distribution of water cluster sizes that fill in the spaces naturally occurring in the acetonitrile liquid. Because water forms a three-dimensional hydrogen bond network, these water clusters are not confined to the small vacancies that are present in bulk acetonitrile, but coalesce into larger clusters that have three or more coordination shells which imply correlation lengths on the order of 0.6 nm to 0.7 nm for $T = 297$ K. The correlation length decreases in size with increasing temperature.

The results for the equimolar case, where two system sizes were examined, indicate that the microheterogeneity does not take the form of isolated clusters. Instead there are interpenetrating regions that are rich in water and in acetonitrile. These regions extend over the volume of the fluid. The composition correlation functions (Figure 6) indicate that the texture of these interpenetrating regions has a length scale on the order of 0.5−1 nm.

This clustering feature is not thought to be the dominant feature leading to retention in RPLC. Instead, the properties of the long chain molecules forming the stationary phase are felt to be more important. However, the clustering properties of these mixtures, and in particular the tendency for water to avoid interfaces, have been shown to provide a thermodynamically favored environment for solutes such that contact of the solute with the stationary phase is enhanced.[3]

References and Notes

(1) Klatte, S. J.; Beck, T. L. *J. Phys. Chem.* **1996**, *100*, 5931.

(2) Beck, T. L.; Klatte, S. J. In *Unified Chromatography*; Chester, T., Parker, J., Eds.; (American Chemical Society: Washington, D.C., 1999).

(3) Slusher, J. T.; Mountain, R. D. *J. Phys. Chem.* **1999**, *103*, 1354.

(4) Snyder, L. R., Kirkland, J. J. *Introduction to Modern Liquid Chromatography*, 2nd ed.; Wiley and Sons: New York, 1979).

(5) Stalcup, A. M.; Martire, D. E.; Wise, S. A. *J. Chromatogr.* **1988**, *442*, 1.

(6) Naberukhin, Y. I.; Rogov, V. A. *Russ. Chem. Rev.* **1971**, *40*, 207.

(7) Wakisaka, A.; Shimizu, Y.; Nishi, N.; Tomumaru, K.; Sakuragi, H. *J. Chem Soc. Faraday Trans.* **1992**, *88*, 1129.

(8) Wakisaka, A.; Takahashi, S.; Nishi, N. *J. Chem. Soc., Faraday Trans.* **1995**, *91*, 4063.

(9) Kirkwood, J. G.; Buff, F. P. *J. Chem. Phys.* **1951**, *19*, 774.

(10) Ben-Naim, A. *Hydrophobic Interactions*; Plenum Press: New York, 1980; pp 78−83.

(11) Matteoli, E.; Lepori, L. *J. Chem. Phys.* **1984**, *80*, 2856.

(12) Marcus, Y.; Migron, Y. *J. Phys. Chem.* **1991**, *95*, 400.

(13) Takamuku, T.; Tabata, M.; Yamaguchi, A.; Nishimoto, J.; Kumamoto, M.; Wakita, H.; Yamaguchi, T. *J. Phys. Chem. B* **1998**, *102*, 8880.

(14) Bergman, D. L.; Laaksonen, A. *Phys. Rev. E* **1998**, *58*, 4706.

(15) Mountain, R. D. *J. Chem. Phys.* **1985**, *82*, 4236.

(16) Martyna, G. J.; Klein, M. L.; Tuckerman, M. *J. Chem. Phys.* **1992**, *97*, 2635.

(17) Sonnenschein, R. *J. Comput. Phys.* **1985**, *59*, 347.

(18) Rapaport, D. C. *J. Comput. Phys.* **1985**, *60*, 306.

(19) Cunningham, G. P.; Vidulich, G. A.; Kay, R. L. *J. Chem. Eng. Data* **1967**, *12*, 336.

(20) Lebowitz, J. L.; Percus, J. K. *Phys. Rev.* **1961**, *122*, 1675.

(21) Münster, A. *Statistical Thermodynamics*; Springer-Verlag: New York, 1969; Vol. 1, pp 343−344.

(22) Berendsen, H. J. C.; Grigera, J. R.; Straatsma, T. P. *J. Phys. Chem.* **1987**, *91*, 6269.

(23) Edwards, D. M. F.; Madden, P. A.; McDonald, I. R. *Mol. Phys.* **1984**, *51*, 1141.

(24) Mountain, R. D. *J. Chem. Phys.* **1997**, *107*, 3921.

(25) Watanabe, K.; Klein, M. L. *Chem. Phys.* **1989**, *131*, 157.

(26) Wallqvist, A.; Mountain, R. D. In *Reviews of Computational Chemistry*; Lipkowitz, K. B., Boyd, D. B., Ed.; Wiley-VCH: New York, 1999; Vol. 13, pp 183−247.

(27) Kiyohara, K.; Gubbins, K. E.; Panagiotopoulos, A. Z. *Mol. Phys.* **1998**, *94*, 803.

(28) Jedlovszky, P.; Richardi, J. *J. Chem. Phys.* **1999**, *110*, 8019.

(29) Sangster, M. J. L.; Dixon, M. *Adv. Phys.* **1976**, *25*, 247.

(30) Geiger, A.; Stillinger, F. H.; Rahman, A. *J. Chem. Phys.* **1970**, *70*, 4185.

(31) Mountain, R. D. *J. Chem. Phys.* **1999**, *110*, 2109.

(32) Goldstein, H. *Classical Mechanics*; Addison-Wesley Publishing Co.: Reading, MA, 1950.

(33) Bhatia, A. B.; Thornton, D. E. *Phys. Rev. B* **1970**, *2*, 3004.

(34) Faber, T. E. *An Introduction to the Theory of Liquid Metals* Cambridge University Press: London, 1972; pp 435−441.

(35) Mountain, R. D. *Mol. Phys.* **1986**, *59*, 857.

(36) Zhang, D.; Gutow, J. H.; Eisenthal, K. B. *J. Chem. Soc., Faraday Trans.* **1996**, *92*, 539.

(37) Eaton, G.; Pena-Nuñez, A. S.; Symons, M. C. R.; Ferrario, M.; McDonald, I. R. *Faraday Discuss. Chem. Soc.* **1988**, *85*, 237.

(38) Dunn, W. J.; Nagy, P. I. *J. Phys. Chem.* **1990**, *94*, 2099.

(39) Kovacs, H.; Laaksonen, A. *J. Am. Chem. Soc.* **1991**, *113*, 5596.

(40) Hummer, G.; Garde, S.; García, A. E.; Pohorille, A.; Pratt, L. R. *Proc. Natl. Acad. Sci.* **1996**, *93*, 8951.

(41) Crooks, G. E.; Chandler, D. *Phys. Rev. E* **1997**, *56*, 4217.

(42) Armitage, D. A.; Blandamer, M. J.; Foster, M. J.; Hidden, N. J.; Morcom, K. W.; Symon, M. C. R.; Wooten, M. J. *Trans. Faraday Soc.* **1968**, *64*, 1193.

(43) Chieux, F.; Ruppersberg, H. *J. Phys. Colloque C8* **1980**, *41*, 145.